

## New Electrohydrodynamic Flow Caused by the Onsager Effect

J. C. Ryu, H. J. Park, J. K. Park, and K. H. Kang\*

*Department of Mechanical Engineering, Pohang University of Science and Technology,  
San 31, Hyoja-dong, Pohang 790-784, Republic of Korea*  
(Received 20 February 2009; published 9 March 2010)

We report a new type of electrohydrodynamic (EHD) flow generated around a circular cylinder and a spherical particle in a dielectric liquid under dc and ac electric fields. The EHD flow is observed for various combinations of dielectric liquids and polar additives. We suggest that the EHD flow is caused by a gradient of electrical conductivity produced by a nonuniform electric field and subsequent generation of free charge in the bulk liquid. Analytical and numerical analyses which are based on the leaky-dielectric model show good agreement with experimental results.

DOI: [10.1103/PhysRevLett.104.104502](https://doi.org/10.1103/PhysRevLett.104.104502)

PACS numbers: 47.65.-d, 47.57.jd

A dielectric liquid is often preferred as a host fluid of a colloidal system under an electric field because one can utilize the full benefits of a strong electric field with little concern for occurrence of electrolysis. Hence, dielectric liquids have been employed in many practical applications such as electrorheological fluids [1], electrophoretic deposition [2], and electrophoretic display [3]. Nonetheless, the dynamics of colloidal particles in dielectric liquids is poorly understood compared to that in aqueous solutions. In colloidal systems under an electric field, electrohydrodynamic (EHD) flows often occur in the bulk liquid or near colloidal particles and electrodes [4]. It can be troublesome, but it can be utilized in such applications as pattern formation and self-assembly of nanoparticles and microparticles [5]. There are many phenomena concerning the dynamics of colloidal particles in dielectric liquids under electric fields which are not fully explained yet, such as the dynamics of fibrillation in electrorheology [6], the driving force for fast lateral migration in electrophoretic displays [7], and collective behaviors of particles in suspension [8]. Those phenomena are highly likely to be related to the EHD flows. Therefore, to understand and control the dynamics of dielectric-liquid-based colloidal systems, fundamental studies on EHD flow are required.

In this Letter, we report a novel EHD flow which occurs near the objects immersed in dielectric liquids containing small amounts of polar additives. We used a conventional particle image velocimetry technique to visualize the EHD flow generated around a circular cylinder and a spherical particle. The application of a strong electric field perturbs initial dissociation-recombination equilibrium between ion pairs and free ions, thus producing a substantial increase in electrical conductivity. This effect is usually referred to as the Onsager effect. We suggest that the EHD flow is generated due to Onsager effect and a conductivity gradient caused by a nonuniform electric field. We call this type of flow the nonuniform-field EHD (NUF EHD) flow. Analytical and numerical solutions are obtained and verified by comparison with experimental results. We discuss the effect of electric-field strength,

system size, and ac frequency on velocity and pattern of NUF EHD flow.

The experimental cell consists of two parallel glass plates coated with indium tin oxide, in which the gap size  $h$  can be controlled. The circular cylinder was placed in the middle of the electrodes with its axis parallel to the two plates. The spherical particle was placed on the surface of the lower electrode. In practical applications, colloidal systems of dielectric liquids generally contain various polar additives. For example, oil-soluble surfactants are added as dispersants to prevent agglomeration of particles, and alcohols and oil-soluble salts are added for fine adjustment of the electrical properties of fluids [9]. As will be discussed, the polar additives are important in generating the EHD flows. We conducted experiments with various combinations of dielectric liquids and polar additives [10]. Fluorescent polystyrene spheres with a diameter  $d$  of  $7\ \mu\text{m}$  were suspended in dielectric liquids as flow tracers. A sheet of laser beam was illuminated to observe, by using a microscope, the flows in a cross section around the cylinder and the sphere.

In dodecane solution mixed with 5 wt % of Span 85, flow patterns were usually symmetric and regular around cylinders of tungsten (highly conductive) and Teflon (poorly conductive) [Figs. 1(a) and 1(b)]. The flow structure is different for the two cases. The flow direction is from the equator ( $\theta = 90^\circ$ ) to the pole regions ( $\theta = 0^\circ, 180^\circ$ ) near the cylinders. In the cases of glass and poly(methyl methacrylate) spheres [Figs. 1(c) and 1(d)], the flow directions of the two large vortices located at the upper part of the sphere are identical to those of the circular cylinders. The maximum flow speed is 1–3 mm/s for all cases. The flow velocity generally decreased with applied frequency  $f$  and eventually stopped above about  $f = 1$  kHz. Flow patterns are little affected by the frequency for the cylinders, while slightly affected around the substrate for the spheres.

The flow patterns of both cylinders and spheres seldom change when a dc electric field is applied instead of an ac field. In addition, a similar flow appears when the diameter of the glass particle is reduced to 200 and 400  $\mu\text{m}$ . We

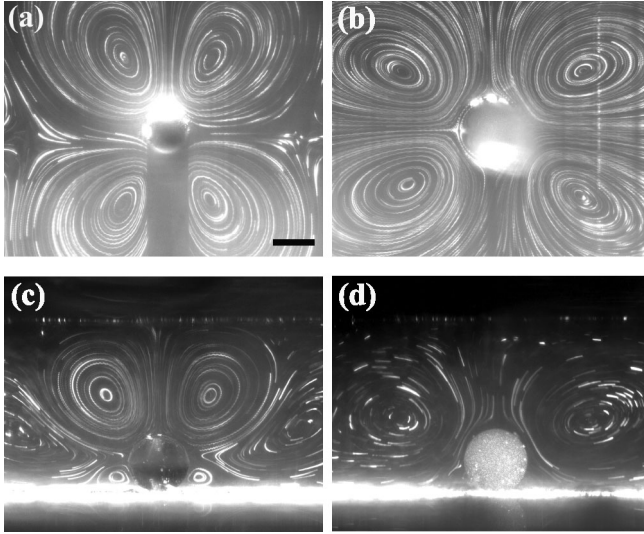


FIG. 1. Streamlines around circular cylinders ( $h = 5$  mm,  $E_0 = 5$  kV/cm,  $f = 30$  Hz) and spherical particles ( $h = 2.5$  mm,  $E_0 = 5$  kV/cm,  $f = 40$  Hz) immersed in dodecane solution mixed with 5 wt% of Span 85. (a) Tungsten cylinder,  $d = 500$   $\mu\text{m}$ , (b) Teflon cylinder,  $d = 770$   $\mu\text{m}$ , (c) glass sphere,  $d = 750$   $\mu\text{m}$ , and (d) polymethyl methacrylate sphere,  $d = 750$   $\mu\text{m}$ .  $E_0 = \Delta V/h$  in which  $\Delta V$  is the root-mean-square voltage applied between the two electrodes. All the photos are in the same scale. Scale bar is 500  $\mu\text{m}$ .

obtained similar results for various combinations of dielectric liquids and polar additives [10]. No flow appeared up to  $E_0 = 30$  kV/cm when we used pure dielectric liquids without additives, which means that the additives play an important role in generating the EHD flow.

The origin of the NUF EHD flow cannot be explained in terms of conventional electrokinetics. In a strong electrolyte solution, which is usually aqueous, conventional electro-osmotic flow (EOF) and induced-charge electro-osmosis (ICEO) are generated [11]. However, conventional EOF is usually not generated for an ac field. The flow direction of the ICEO is always toward the particle at both pole regions ( $\theta = 0^\circ, 180^\circ$ ) (e.g., Fig. 1 in Ref. [11]), irrespective of material properties [12,13], which is evidently *opposite* to those shown in our Fig. 1. As will be described, the flow velocity of present EHD flow is proportional to  $E^3$ , while the EOF and ICEO are proportional to  $E$  and  $E^2$ , respectively. Moreover, the ICEO is usually very weak for dielectric materials [13], whereas the present flow is prevalent for both dielectric materials and conducting materials. Consequently, the EOF and ICEO are excluded from our consideration.

The origin of NUF EHD flow also cannot be explained in terms of conventional EHD flows. EHD flows in a weak electrolyte, such as considered in this work, are classified as the injection, conduction, and induction EHD flows according to the origin of the electrical charge [14]. For injection EHD flows, space charges are generated by the ions injected by a needle-type electrode. For conduction

EHD flows, these charges are generated by a heterocharge layer that forms in the vicinity of an electrode (see, for more details, Ref. [14]). However, these types of EHD flow are generated only for dc case. Furthermore, we confirmed that an identical flow pattern [Fig. 1] was still generated under the same conditions even when the electrode was coated by a 5- $\mu\text{m}$  insulating film of parylene-C, which might prevent or reduce the generation of charge. Thus, injection EHD flow and conduction EHD flow are also excluded.

Induction EHD flow relies on induced free charges in the bulk liquid. Electrothermal flows [15] and the electrokinetic instability [16] are the typical examples of this type of flow. In weak electrolyte systems, such an EHD flow is generated only when the temperature gradient is externally imposed because the temperature rise by Joule heating in a dielectric liquid is usually not significant [14]. In what follows, we suggest a new charge-induction mechanism which is the origin of the NUF EHD.

According to Onsager's theory, conductivity is proportional to electric-field strength ( $E$ ) because the dissociation rate of uncontrollable chemical impurities in a dielectric liquid increases with electric-field strength [17,18]. Hence, any nonuniformity in electric-field strength can produce a gradient of conductivity and generate electrical charges. Such a field-enhanced dissociation process can be promoted by adding polar additives such as surfactants and alcohols. The polar molecules screen the Coulombic interactions between ions by means of ion-dipole interactions [18,19]. As a consequence, the ion recombination rate is significantly reduced, which leads to a dramatic increase in conductivity. According to our measurements, the dc conductivity of pure dielectric liquids is increased  $10^4$  times by adding just a few wt% of additives [10]. The conductivity of various mixtures used in this study is almost linearly proportional to applied electric-field strength as well as to the concentration of additives, while the electrical permittivity  $\epsilon$  showed little dependence on electric-field strength [10]. We suggested that the electrical conductivity  $\sigma(E)$  of the mixtures can be approximately represented by

$$\sigma(E) = \bar{\sigma}(1 + \gamma E). \quad (1)$$

Here,  $\bar{\sigma}$  represents the conductivity of fluid without an electric field, and  $\bar{\sigma}$  is a function of additive concentration. The constant  $\gamma$  is determined empirically between  $2.25 \times 10^{-5}$  and  $3.01 \times 10^{-5}$  cm/V, for most mixtures considered in this work, which is consistent with theoretical values [10]. As a result, a variation of electric-field strength of, for example,  $E = 10$  kV/cm, may change conductivity by about 20% for typical dielectric-liquid-additive mixtures. It follows that a nonuniform electric field can somehow contribute to charge separation in a bulk fluid, which is essential for generation of an EHD flow.

Before carrying out mathematical analysis, we checked whether such a field-enhanced charge-generation mechanism is likely to generate such fast flows [Fig. 1]. Under dc electric fields with constant  $\epsilon$ , the free charge density  $\rho_f$  is

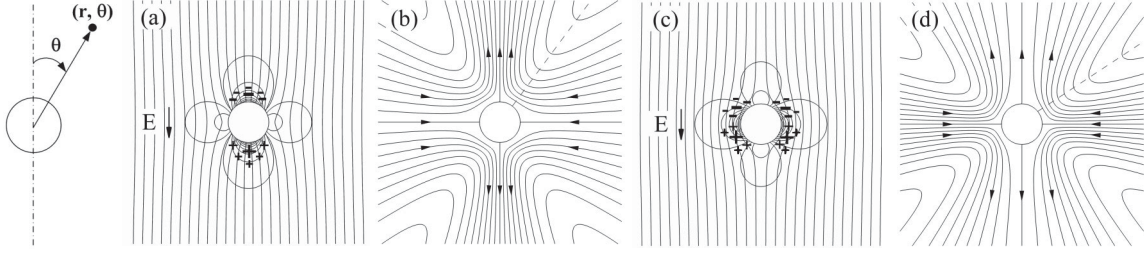


FIG. 2. Mechanism of the NUF EHD flow for conducting cylinder (a),(b) and dielectric cylinder (c),(d). Panels (a) and (c) show the electric-field lines (vertical lines), conductivity contours (circular arcs), and sign of free charges; panels (b) and (d) show the streamlines. The figures are based on the analytical solution for dc case, where  $\bar{\sigma} = 6.15 \times 10^{-9}$ , and the dielectric constant of fluid  $\epsilon_r = 2.01$ .

related to the conductivity gradient as [14]

$$\rho_f = -\frac{\epsilon \nabla \sigma \cdot \mathbf{E}}{\sigma} = -\epsilon \nabla \ln \sigma \cdot \mathbf{E}, \quad (2)$$

where  $\mathbf{E}$  is the electric field. If we assume that  $0 < \gamma E \ll 1$ , Eq. (2) becomes  $\rho_f \cong -\epsilon \gamma (\nabla E) \cdot \mathbf{E}$ . We can estimate the Coulombic force per unit volume on an infinitesimal fluid element as  $\rho_f \mathbf{E} \sim \epsilon \gamma E^3/a$ , where  $a$  represents the radius of a cylinder or sphere. If the Coulombic force is balanced by the viscous force, the characteristic flow velocity is estimated as  $u_c \sim \epsilon \gamma E^3 a / \mu$ , where  $\mu$  is the viscosity of fluid. The calculated value is  $u_c \sim 3$  mm/s for the conditions in Fig. 1, which is consistent with experimental results (1–3 mm/s).

To verify the concept rigorously, we solved the Stokes equation analytically and the Navier-Stokes equation numerically [20]. Under the quasielectrostatic assumption [21], the electric field is described by the Poisson equation ( $\nabla^2 \phi = -\rho_f/\epsilon$ ) and charge conservation equation ( $\partial \rho_f / \partial t + \nabla \cdot \mathbf{J} = 0$ ). The current density  $\mathbf{J}$  is assumed to satisfy the modified Ohm's law of  $\mathbf{J} = \sigma(E)\mathbf{E}$ . Under the creeping flow approximation, analytical solutions of the electric potential  $\phi$  and the streamline  $\psi$  for a circular cylinder located inside an unbounded domain are obtained by using a perturbation method [20]. The leading order electrical potential  $\phi_0$  in the fluid side becomes  $\phi_0(r, \theta) = \text{Re}\{E_\infty a \hat{r} \cos\theta (1 + \beta \hat{r}^{-2}) e^{j\omega t}\}$ , where  $\beta = (\bar{\sigma}_0 - \bar{\sigma}') / (\bar{\sigma}_0 + \bar{\sigma}')$ ,  $E_\infty$  is the electric-field strength at far field,  $\hat{r} = r/a$ ,  $j = \sqrt{-1}$ , and  $\omega = 2\pi f$ . Hereafter,  $\bar{\sigma}_0 = \bar{\sigma} + j\omega\epsilon$ ,  $\bar{\sigma}' = \sigma' + j\omega\epsilon'$ , and the prime denotes the cylinder (or sphere). The stream function for a conducting cylinder ( $\psi_+$ ) and a perfect dielectric cylinder ( $\psi_-$ ) becomes

$$\begin{aligned} \psi_\pm(r, \theta) = & \frac{\gamma}{240\pi c_\pm} \frac{1}{1 + \Omega^2} \frac{\epsilon a^2 E_\infty^3}{\mu} \\ & \times [(58 - 120\hat{r}^{-2} \ln\hat{r} - 57\hat{r}^{-2} - \hat{r}^{-6}) \sin 2\theta \\ & + (\pm 10 \mp 20\hat{r}^{-2} \pm 10\hat{r}^{-4}) \sin 4\theta], \end{aligned} \quad (3)$$

where  $\Omega = \epsilon\omega/\bar{\sigma}$ ,  $c_+ = 2$ , and  $c_- = 1.63$ . The solution for the dielectric cylinder ( $\psi_-$ ) is valid for  $2\omega\bar{\sigma}\epsilon'/[\bar{\sigma}^2 + \omega^2(\epsilon^2 - \epsilon'^2)] \ll 1$  [e.g., for the condition in Fig. 2(b),  $f \ll 30$  Hz]. For these two limiting cases, the velocity vec-

tors have only the  $r$  component at far field, and their directions change at  $\theta \cong 36.6^\circ$  for the conducting cylinder and at  $\theta \cong 53.4^\circ$  for the dielectric cylinder (see dashed lines in Fig. 2). This result may explain why the centers of vortices are shifted toward  $\theta = 90^\circ$  for the case of the Teflon cylinder compared to that of the tungsten cylinder [Fig. 1].

Let us look into the full analytical solution plotted in Fig. 2 for the conducting and dielectric cylinders. For the conducting cylinder, for example, the electric field is strongest at the poles ( $\theta = 0^\circ, 180^\circ$ ) and weakest at the equator ( $\theta = 90^\circ$ ) [Figs. 2(a) and 2(b)]. Because the gradient of the electric field is greatest near  $\theta = 0^\circ$  and  $180^\circ$ , negative charges are produced near  $\theta = 0^\circ$  and positive charges near  $\theta = 180^\circ$ . Therefore, the Coulombic force directs away from the cylinder at both poles, and subsequently the flow near the cylinder moves from the equator to the pole. Significantly, as mentioned earlier, this flow occurs in a direction *opposite* of the ICEO flows. The flow patterns are consistent with the experimental results [Figs. 1(a) and 1(b)]. The full numerical solution for the case in Figs. 1(a) and 1(c) confirmed that the analytical solution agrees very well in flow pattern with our numerical solution obtained for a nearly unbounded domain [20]. The experimental and numerical results show a reasonable agreement in flow pattern and direction [Fig. 3].

When  $E \lesssim 9$  kV/cm, the average velocity is proportional to  $E_0^3 a$  [Fig. 4(a)], as predicted by the scaling analysis. Here, the average velocity is defined as the average of

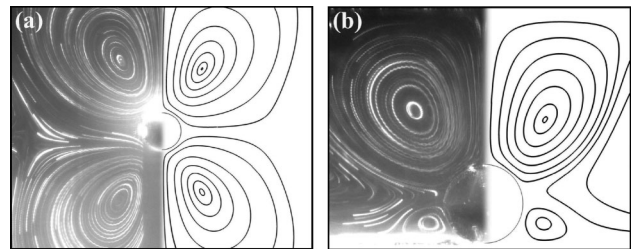


FIG. 3. Comparison of numerical simulation (right) with experimental results (left): (a) tungsten cylinder and (b) spherical glass particle. The numerical simulation was executed under the same conditions as those of Figs. 1(a) and 1(c).

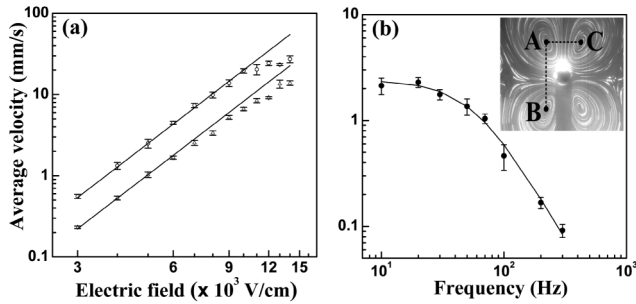


FIG. 4. The dependency of average flow velocity on (a) electric-field strength ( $f = 30$  Hz) and (b) frequency ( $E_0 = 5 \times 10^3$  V/cm) for the case of tungsten cylinder. All the data are plotted to logarithmic scale. In (a), circles and triangles are for  $d = 500 \mu\text{m}$  and  $d = 250 \mu\text{m}$ , respectively, and solid lines represent  $E^3$  curves. In (b), solid lines represent theoretical values. In the inset of (b), the two lines  $\overline{AB}$  and  $\overline{AC}$  connect the center of the vortices.

vertical velocity across the line  $\overline{AB}$  and horizontal velocity across the line  $\overline{AC}$  [Fig. 4(b), inset]. Such agreements in scaling behavior and flow pattern between prediction and experiment strongly support the suggestion that the present EHD flow originates from the field-dependent conductivity. On the other hand, there is a discrepancy between the theory and experimental results when  $E \geq 9$  kV/cm. This discrepancy is conjectured to be caused by the convective flux of free charges around the bodies. We carefully monitored the voltage and current signals, but there was no particular sign of ion injection from electrodes.

For a conducting cylinder, the velocity decreases with frequency as  $(1 + \Omega^2)^{-1}$ . The characteristic time for the electric field is determined by  $\Omega = 1$ , which corresponds to about  $f = 55$  Hz for the tungsten cylinder and is consistent with the experimental results [Fig. 4(b)]. Because the charge density is proportional to  $\nabla \ln \sigma$  for a given electric field, the flow velocity is independent of  $\bar{\sigma}$  for dc cases. When we increased the concentration of Span 85 to 5 wt% to verify the effect of  $\bar{\sigma}$  for an ac case, the flow pattern is rather insensitive to additive concentration while the average velocity tends to increase with additive concentration slightly. This is consistent with the theoretical prediction that the conductivity contributes to flow velocity in the form of  $(1 + \epsilon^2 \omega^2 / \bar{\sigma}^2)^{-1}$  in Eq. (3).

It should be noted that the flow velocity is scaled as  $E^3$  because it is quite different from the conventional EHD flows, which is usually scaled as  $E^2$ . More importantly, the flow velocity is proportional to the radius  $a$  of the cylinder or sphere, so that the velocity will not be reduced as much as  $a$  is reduced. Our preliminary analysis for hydrodynamic interaction due to the NUF EHD flow between two spherical particles indicates that the hydrodynamic interaction is at least comparable to that of dipole-dipole interactions. This implies that NUF EHD flow can be a

dominant factor which governs the dynamic behavior of colloidal particles in dielectric liquids under electric fields.

In summary, we discovered an EHD flow in dielectric liquids mixed with polar additives which appears to be due to the field dependence of conductivity caused by the screening effect of polar additives. The NUF EHD flow will become a key to understanding and controlling the dynamics of dielectric-liquid-based colloidal systems. Also, the NUF EHD flow itself may have broad applications including electromotive pumps and micromixers in microfluidic devices.

This work was supported by the Korea Research Foundation (KRF) grant funded by the Korea government (MEST) (R0A-2007-000-20098-0 and R01-2006-000-10657-0) and the POSTECH Research Fund. The authors acknowledge Professor T. M. Squires and Professor H. K. Pak for fruitful discussions.

\*khkang@postech.ac.kr

- [1] M. Parthasarathy and D. J. Klingenberg, *Mater. Sci. Eng.*, **R 17**, 57 (1996).
- [2] L. Besra and M. Liu, *Prog. Mater. Sci.* **52**, 1 (2007).
- [3] B. Comiskey *et al.*, *Nature (London)* **394**, 253 (1998).
- [4] P. J. Sides, *Langmuir* **17**, 5791 (2001); M. Trau, D. A. Saville, and I. A. Aksay, *Langmuir* **13**, 6375 (1997); W. D. Ristenpart, I. A. Aksay, and D. A. Saville, *Phys. Rev. Lett.* **90**, 128303 (2003).
- [5] M. Trau *et al.*, *Nature (London)* **374**, 437 (1995); M. V. Sapozhnikov *et al.*, *Phys. Rev. Lett.* **90**, 114301 (2003).
- [6] T. Hao, *Adv. Colloid Interface Sci.* **97**, 1 (2002).
- [7] P. Murau and B. Singer, *J. Appl. Phys.* **49**, 4820 (1978); J. H. Kim *et al.*, *Langmuir* **21**, 10941 (2005).
- [8] Y. Solomentsev, M. Bohmer, and J. L. Anderson, *Langmuir* **13**, 6058 (1997); Y. Solomentsev *et al.*, *Langmuir* **16**, 9208 (2000).
- [9] I. D. Morrison, *Colloids Surf. A* **71**, 1 (1993).
- [10] J. K. Park *et al.*, *J. Phys. Chem. B* **113**, 12271 (2009).
- [11] M. Z. Bazant and T. M. Squires, *Phys. Rev. Lett.* **92**, 066101 (2004).
- [12] G. Yossifon, I. Frankel, and T. Miloh, *Phys. Fluids* **19**, 068105 (2007).
- [13] J. C. Ryu, H. J. Park, J. K. Park, and K. H. Kang (unpublished), available on request.
- [14] A. Ramos, in *Microfluidic Technologies for Miniaturized Analysis Systems*, edited by S. Hardt and F. Schonfeld (Springer, New York, 2007), p. 59.
- [15] A. Gonzalez *et al.*, *J. Fluid Mech.* **564**, 415 (2006).
- [16] H. Lin *et al.*, *Phys. Fluids* **16**, 1922 (2004).
- [17] L. Onsager, *J. Chem. Phys.* **2**, 599 (1934).
- [18] A. I. Zhakin, in *Electrohydrodynamics*, edited by A. Castellanos (Springer Verlag, Wien, 1998), p. 83.
- [19] A. S. Dukhin and P. J. Goetz, *J. Electroanal. Chem.* **588**, 44 (2006).
- [20] H. J. Park, J. C. Ryu, J. M. Oh, and K. H. Kang (to be published).
- [21] D. A. Saville, *Annu. Rev. Fluid Mech.* **29**, 27 (1997); A. Castellanos *et al.*, *J. Phys. D* **36**, 2584 (2003).